

Accepted Manuscript

Osteoclast differentiation from human blood precursors on biomimetic calcium-phosphate substrates

Gabriela Ciapetti, Gemma di Pompo, Sofia Avnet, Desirée Martini, Anna Diez-Escudero, Edgar B. Montufar, Maria-Pau Ginebra, Nicola Baldini

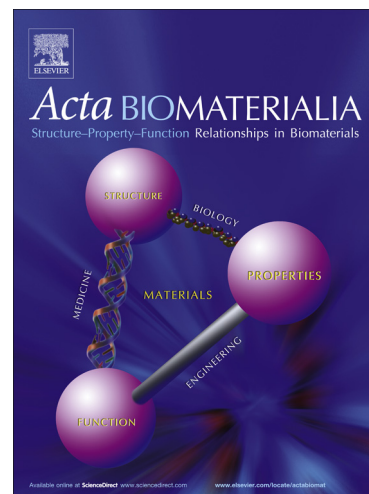
PII: S1742-7061(16)30681-X
DOI: <http://dx.doi.org/10.1016/j.actbio.2016.12.013>
Reference: ACTBIO 4594

To appear in: *Acta Biomaterialia*

Received Date: 15 July 2016
Revised Date: 8 November 2016
Accepted Date: 6 December 2016

Please cite this article as: Ciapetti, G., di Pompo, G., Avnet, S., Martini, D., Diez-Escudero, A., Montufar, E.B., Ginebra, M-P., Baldini, N., Osteoclast differentiation from human blood precursors on biomimetic calcium-phosphate substrates, *Acta Biomaterialia* (2016), doi: <http://dx.doi.org/10.1016/j.actbio.2016.12.013>

This is a PDF file of an unedited manuscript that has been accepted for publication. As a service to our customers we are providing this early version of the manuscript. The manuscript will undergo copyediting, typesetting, and review of the resulting proof before it is published in its final form. Please note that during the production process errors may be discovered which could affect the content, and all legal disclaimers that apply to the journal pertain.



OSTEOCLAST DIFFERENTIATION FROM HUMAN BLOOD PRECURSORS ON BIOMIMETIC CALCIUM-PHOSPHATE SUBSTRATES

Gabriela Ciapetti ^{a,1,*}, Gemma di Pompo ^{a,b,1}, Sofia Avnet ^a, Desirée Martini ^b, Anna Diez-Escudero ^c, Edgar B. Montufar ^c, Maria-Pau Ginebra ^{c,d}, Nicola Baldini ^{a,b}

^a Orthopaedic Pathophysiology and Regenerative Medicine Unit, Istituto Ortopedico Rizzoli, Bologna, Italy

^b Department of Biomedical and Neuromotor Sciences, University of Bologna, Italy

^c Biomaterials, Biomechanics and Tissue Engineering Group, Department of Materials Science and Metallurgy, Technical University of Catalonia, BarcelonaTech (UPC), Barcelona, Spain

^d Institute for Bioengineering of Catalonia, Barcelona, Spain

¹ The first two authors have equal contributions.

gabriela.ciapetti@ior.it

gemma.dipompo@ior.it

sofia.avnet@ior.it

desiree.martini@unibo.it

anna.diez-escudero@upc.edu

edgar.montufar@upc.edu

mariapau.ginebra@upc.edu

nicola.baldini@ior.it

Corresponding Author: Gabriela Ciapetti, MSc
SSD Fisiopatologia Ortopedica e Medicina Rigenerativa, Istituto
Ortopedico Rizzoli, via di Barbiano 1/10, 40136 Bologna, ITALY
Phone: +39 051 6366896
Fax: +39 051 6366974
e-mail : gabriela.ciapetti@ior.it

OSTEOCLAST DIFFERENTIATION FROM HUMAN BLOOD PRECURSORS ON BIOMIMETIC CALCIUM-PHOSPHATE SUBSTRATES

Abstract

The design of synthetic bone grafts to foster bone formation is a challenge in regenerative medicine. Understanding the interaction of bone substitutes with osteoclasts is essential, since osteoclasts not only drive a timely resorption of the biomaterial, but also trigger osteoblast activity.

In this study, the adhesion and differentiation of human blood-derived osteoclast precursors (OCP) on two different micro-nanostructured biomimetic hydroxyapatite materials consisting in coarse (HA-C) and fine HA (HA-F) crystals, in comparison with sintered stoichiometric HA (sin-HA, reference material), were investigated. Osteoclasts were induced to differentiate by RANKL-containing supernatant using cell/substrate direct and indirect contact systems, and calcium (Ca^{++}) in culture medium was measured.

We observed that OCP adhered to the experimental surfaces, and that osteoclast-like cells formed at a rate influenced by the micro- and nano-structure of HA, which also modulate extracellular Ca^{++} .

Qualitative differences were found between OCP on biomimetic HA-C and HA-F and their counterparts on plastic and sin-HA. On HA-C and HA-F cells shared typical features of mature osteoclasts, i.e. podosomes, multinuclearity, tartrate acid phosphatase (TRAP)-positive staining, and TRAP5b-enzyme release. However, cells were less in number compared to those on plastic or on sin-HA, and they did not express some specific osteoclast markers. In conclusion, blood-derived OCP are able to attach to biomimetic and sintered HA substrates, but their subsequent fusion and resorptive activity are hampered by surface micro-nano-structure. Indirect cultures suggest that fusion of OCP is sensitive to topography and to extracellular calcium.

Key-words osteoclasts; hydroxyapatite; differentiation; topography; ionic exchange; bone resorption.

1. INTRODUCTION

During implant integration toward a successful clinical outcome, surfaces of orthopaedic materials interact with host bone cells, triggering a chain of biological events where osteoclasts and osteoblasts are involved in the replacement of damaged bone by new bone [1].

Synthetic materials for bone replacement are widely tested for their osteoconduction and/or osteoinduction, with substrates hosting osteoblasts or osteoblastic cell lines scored as promising materials. But the replacement of bone substitutes with newly formed bone implies that the material is gradually removed to leave space for new bone tissue, and recent research has shed light on the close osteoclast/osteoblast cooperation for bone formation and remodelling. Osteoclasts have been shown to secrete products to promote osteoblast precursor recruitment and differentiation and thereby promote bone formation [2]. Therefore, understanding the nature of the interactions of the different biomaterials used as synthetic bone grafts and osteoclasts is of paramount importance.

Osteoclasts, both from humans and mice, have been tested using *in vitro* protocols and shown to be able to resorb hydroxyapatite (HA) by imprinting pits on the HA surface [3,4]. Murine RAW.246.7 or mouse marrow-derived cells are largely employed in studies of osteoclasts on ceramics [5-7], with only a few publications addressing osteoclast differentiation of human monocytes on ceramic substitutes [8,9]. These studies have shown that osteoclasts are sensitive to different material properties, such as chemical composition and topography. However, the most crucial parameters of this interaction have not been fully identified.

In this work we investigated the effect of the composition and surface topography of HA substrates on osteoclast differentiation of human blood precursors. Biomimetic HA substrates can be obtained by low-temperature setting reactions, where a calcium deficient hydroxyapatite (Ca/P ratio = 1.5) is formed through the hydrolysis of α -tricalcium phosphate (α -TCP) [10], which is very similar to the mineral phase of bone, in terms of chemical composition, crystallinity and specific surface area. We have previously shown that the microstructure of these materials can be reliably controlled by tuning the particle size of the starting powders [11,12], obtaining materials with the same chemistry and different surface topographies [13].

In addition, sintered stoichiometric HA (Ca/P ratio = 1.67) with surface topography quite different from that obtained in biomimetic HA was included in the study. This type of stoichiometric HA is also commonly used as bone filler in clinics and is typically fabricated by high temperature treatments. In order to better understand the effect on the cells of the ionic

exchange between the material and the cell culture medium, osteoclast precursors were also exposed to material extracts.

To mimic the bone tissue microenvironment, peripheral blood mononuclear cells (PBMC) were isolated and induced to differentiate to osteoclasts on biomimetic and sintered stoichiometric HA substrates by RANKL-containing supernatants from osteoblast cultures. This method closely mimics the bidirectional osteoclast/osteoblast interaction occurring *in vivo* at the sites of bone remodeling [14].

2. MATERIALS AND METHODS

2.1. Synthesis and characterisation of biomimetic HA substrates with different topographies

Biomimetic HA substrates with identical composition, but different micro/nanostructural features were obtained by low-temperature setting of a α -TCP cement, using starting powders with different particle sizes, as previously reported [11].

Briefly, α -TCP was obtained by heating in a furnace (Hobersal CNR-58), in air, an appropriate mixture of calcium hydrogen phosphate (CaHPO_4 , Sigma–Aldrich C7263) and calcium carbonate (CaCO_3 , Sigma–Aldrich C4830) at 1400 °C for 2 h followed by quenching in air. Two different sizes of α -TCP powder were prepared following two different milling protocols. The powder with larger size (coarse, C) was milled in an agate ball mill (Pulverisette 6, Fritsch GmbH) with 10 balls ($d = 30$ mm) for 15 min at 450 rpm. The powder with smaller particle size (fine, F) was first milled with 10 balls ($d = 30$ mm) for 60 min at 450 rpm followed by a second milling for 70 min at 500 rpm with 100 balls ($d = 10$ mm). Precipitated hydroxyapatite (2 wt%; Alco 1.02143) was added as a seed in the powder. The cement's liquid phase consisted of an aqueous solution of 2.5 wt % disodium hydrogen phosphate (Na_2HPO_4 , Panreac 131679.1210). A liquid to powder (L/P) ratio of 0.35 ml/g was used to prepare disks of 14 mm diameter and 0.25 mm high in Teflon moulds. The cements were allowed to set in Ringer's solution (0.9 wt.% NaCl) for 7 days at 37 °C to obtain the calcium deficient HA. In addition, stoichiometric HA discs were obtained by sintering in air at 1100 °C for 20 h a pre-compacted mixture of CaHPO_4 and CaCO_3 at 50 MPa, with a calcium to phosphorous ratio of 1.67. Biomimetic HA samples were named HA-C and HA-F in accordance with the powder size used to prepare them, and the stoichiometric HA, used as a reference material for cell cultures, was named sin-HA.

The microstructure on the surface of the samples was observed by scanning electron microscopy (SEM, Zeiss Neon40, 5 kV). A thin gold/palladium layer was deposited on the sample surface through vapour deposition before analysis to enhance conductivity. The surface roughness was characterized by optical interferometry (Veeco Wyko NT1100), using a 50x magnification and a scanned area of 125 x 95 mm². Images were processed using Vision32 software. The specific surface area (SSA) of the samples was determined by nitrogen adsorption (ASAP 2020 Micromeritics) using the Brunauer- Emmett-Teller (BET) method.

2.2 Osteoclast cultures

Peripheral blood mononuclear cells (PBMC), containing the precursors of human osteoclasts, were isolated from buffy coats of healthy voluntary blood donors to the National Blood Transfusion Service. Donation was anonymous, and institutional review board (IRB) approval was not required.

The mononuclear cells were isolated by density centrifugation using Ficoll-Histopaque gradient (Sigma–Aldrich), washed with phosphate-buffered saline (PBS), re-suspended in Dulbecco's Modified Eagle's Medium – High Glucose (DMEM, Euroclone, Milan, Italy) supplemented with 10 % fetal bovine serum (FBS, Euroclone) (complete DMEM), and seeded for the direct and indirect assays.

To induce the differentiation of osteoclast precursor (OCP) the RANKL-containing human osteoblast (HOB) supernatant was used [15,16]. HOB were seeded (1.5×10^4 cells/cm²) in 75-cm² tissue-culture flasks in complete DMEM medium. After reaching 90% confluence, the cell supernatant was collected, centrifuged at 2000g at 4 °C for 10 minutes, and stored at –80°C until use. In both the culture systems the OCP were re-stimulated with 25% HOB supernatant every 3 days with a medium change along the 21-day culture period.

2.2.1 Direct contact assay

The biomimetic HA (HA-C and HA-F) and sintered HA (sin-HA) disks were placed at the bottom of 24 well-polystyrene culture plates (Nalge-Nunc International, Rochester, New York, USA), and were pre-conditioned with complete DMEM, in humidified 5% CO₂ atmosphere at 37°C for 4 days. Then the medium was removed and 6×10^6 cells per cm² were seeded on the preconditioned disks, whereas 3×10^6 cells per cm² were seeded in the tissue culture polystyrene wells (TCPS) and used as controls.

After incubation for 2 h at 37 °C in humidified atmosphere, with 5 % CO₂, the non-adherent cells were removed, and complete DMEM supplemented with 25 % RANKL-containing human

osteoblast supernatant (differentiation medium) was added to adherent cells for the direct contact assay.

Changes in calcium and phosphorus concentration of the culture medium in contact with the HA substrates, with or without cells, were determined at 317.933 and 177.95 nm respectively by Inducted Coupled Plasma – Optical Emission Spectroscopy (ICP-OES, Perkin-Elmer Optima 3200 RL). Ionic concentrations were determined once a week in triplicate for a period of 21 days.

2.2.2 Indirect contact assay

The extracts of the biomimetic and sintered HA were prepared by dipping a disk in 1 ml of complete DMEM at 37 °C in a humidified atmosphere with 5 % CO₂. After 3 days each extract was collected to be used in the indirect contact assay, and new complete DMEM was added to the disk to keep the disk/medium proportion. The extracts were collected using this protocol every 3 days along the whole culture period (21 days).

For the indirect contact assay, cells (3×10^6 per cm²) were seeded on TCPS and after 2 h the non-adherent cells were removed, and the adherent cells were cultured with extracts supplemented with 25% of RANKL-containing human osteoblast supernatant. A culture treated with the differentiating medium only was used as a control.

2.3 Cell morphology

2.3.1 Confocal microscopy

OCPs were fixed in 3.7 % paraformaldehyde/PBS, pH 7.4, at room temperature for 20 min. After a rinse with PBS, permeabilization with 0.5 % Triton X-100 in PBS for 10 min at room temperature and staining using 1:200 Phalloidin–Tetramethylrhodamine B isothiocyanate (Sigma–Aldrich) for 45 min in the dark, the OCP were observed by confocal microscopy (ECLIPSE E600, NIKON Corp.) at 520 nm excitation and 582 nm emission.

2.3.2 Focused Ion Beam-Scanning Electron Microscopy (FIB-SEM)

For FIB - SEM (Zeiss Neon 40) examination of the cells in direct contact test, the disks removed from the culture plates were rinsed with 0.1 M PBS and the OCP fixed with 2 % paraformaldehyde/2 % glutaraldehyde in 0.1 M cacodylate buffer overnight at 4 °C. Following a rinse in 0.1 M cacodylate buffer, each sample was postfixed in 2 % osmium tetroxide (OsO₄) for 2 h at room temperature. Fixed samples were then dehydrated in an ethanol series followed by hexamethyl-disililane drying. The dried samples were covered with a gold-palladium thin film.

After SEM observation, FIB lithography was used to examine the material underlying the cells. Selected cells were sectioned vertically by a Gallium ion beam at 30 keV. First, a thin layer of platinum (Pt) was deposited on the surface by ion-beam assisted deposition in order to reduce the curtaining effect and to obtain a smoother cross-section. Then, a rough milling was performed with a maximum current of 10 nA to quickly remove most of the material up to a depth of approximately 20 μm nearby the region of interest. Finally, a polished cross-section was obtained by subsequently reducing the Gallium beam current from 2 nA down to 500 pA when approaching the Pt layer. This procedure reduced the ion beam damage to the sample and the redeposition effects and allowed observing a cross-section of the cell and the underlying microstructure without any modifications.

2.4 Osteoclast recognition

2.4.1 Tartrate-Resistant Acid Phosphatase and Hoechst staining

Tartrate-resistant acid phosphatase (TRAP) positivity and multinuclearity, i.e. more than 3 nuclei per cell, were used to verify *in situ* monocytes differentiation to mature osteoclasts. For TRAP staining the OCP were fixed with 3 % paraformaldehyde-2 % sucrose for 30 min, permeabilized with Triton 0.5 % in HEPES for 5 min at room temperature, and stained using naphthol AS-BI phosphoric acid and tartrate solution (Acid Phosphatase kit, Sigma–Aldrich) for 60 min at 37 °C.

Cell nuclei were stained by cell incubation with 2.25 $\mu\text{g}/\text{mL}$ of Hoechst 33258 (Sigma–Aldrich) for 10 min in the dark. TRAP stained samples were observed by optical microscopy and the nuclei under fluorescence microscope at 360 nm excitation and 470 nm emission.

2.4.2 Tartrate-Resistant Acid Phosphatase activity

To quantify the cellular tartrate-resistant acid phosphatase isoform 5b (TRAP5b) activity, after 21 days of culture the supernatants of cells grown on HA substrates and TCPS were collected, centrifuged at 400g for 5 min and assayed using the BoneTRAP® Assay kit (Pantec s.r.l., Torino, Italy), according to the manufacturer's instructions.

The concentration of TRAP5b protein in the supernatants was determined by reading the absorbance at 405 nm in a spectrophotometer (Tecan Infinite F200pro, Mannedorf, Switzerland).

Data are expressed as mean concentration (units/L) after subtraction of the corresponding cell-free readout.

2.4.3 Osteoclastic gene expression

Gene expression of the osteoclast markers cathepsin K (CTSK), Matrix Metalloproteinase-9 (MMP-9) and vacuolar-ATPase (v-ATPase) was evaluated by Real-time PCR after 21 days of culture and compared to expression at seeding (day 0).

Total RNA was extracted from cells using TRIzol® (Invitrogen, Carlsbad, CA) according to the manufacturer's protocol, and reverse transcribed. A260/A280 ratio of the prepared total RNA was always ≥ 1.85 . Messenger-RNA expression was evaluated using a Light Cycler instrument (Roche Diagnostics, Indianapolis, IN) and the Universal Probe Library (Roche Applied Science).

Probes and primers were selected using a web-based assay design software (ProbeFinder <http://www.rocheapplied-science.com>). Gene sequences and primers are reported in Table I.

The results were normalized to the 18S ribosomal RNA (rRNA 18s) control housekeeping gene.

2.5 Statistics

Statistical analysis was performed using StatView 5.01 for Windows (SAS Institute Inc, Cary, NC). Mann-Whitney U test was used for the unpaired comparison of two independent variables. Quantitative data were expressed as an arithmetic mean plus or minus the standard error of the mean, and differences were considered significant at P values ≤ 0.05 .

3. RESULTS

3.1 Material characterisation

Biomimetic HA substrates with distinct isotropic topographies were obtained by the hydrolysis of α -TCP powders with different particle size distributions. Detailed characterization of the composition, crystallinity, compressive strength and porosity has been described in previous papers [10,11]. Both materials consisted of the same crystal phase, that is poorly crystalline, calcium-deficient HA.

SEM micrographs, as well as the images obtained by optical interferometry, are shown in Figure 1.

In both HA-F and HA-C substrates the surface topography was complex, composed of spherical-like agglomerates of plate-like crystals of micrometric size (HA-C) or needle-like crystals of nanometric size (HA-F), resulting in a combined micro- and nanotopography, as described in detail in a previous publication [13].

HA-F developed a much finer structure than the HA-C, the average roughness (Ra) being 0.7 ± 0.1 and 1.7 ± 0.2 μm , respectively, for HA-F and HA-C. The SSA was approximately double for HA-F ($33 \text{ m}^2/\text{g}$) in comparison to HA-C ($18 \text{ m}^2/\text{g}$).

In contrast, the surface topography of sin-HA substrates consisted of smooth polyhedral grains of several micrometers, connected by sintering necks with few remaining pores. Although the surface roughness of sin-HA (Ra = 0.6 ± 0.1 μm) was similar to that of HA-F, the SSA was significantly lower than that of biomimetic HA ($0.54 \text{ m}^2/\text{g}$).

X-ray diffraction (data not shown) confirmed the purity and high crystallinity of sin-HA.

3.2 Direct-contact assay

Osteoclast precursors isolated from peripheral blood were found to attach to all the surfaces under assay, and osteoclasts were induced by the differentiation medium, i.e. under the influence of RANKL, the osteoclast differentiating factor produced by osteoblasts. *In situ* osteoclast differentiation on HA-C and HA-F biomimetic substrates was assessed by analyzing morphology, specific markers, and gene expression of osteoclasts. Tissue culture plastic and sin-HA, that are surfaces known as permissive for osteoclast differentiation, were used as control and reference material, respectively. Wherever not specified, the assay was performed after 21 days of culture of OCP on the different substrates.

3.2.1 Morphology

The cytoskeletal actin ring of the cells, indicative of mature osteoclasts, was examined by confocal laser scanning microscopy on samples stained with rhodamine-phalloidin.

A few clusters of cells, 10-20 μm in diameter, with a peripheral actin stain, were observed on both HA-C and HA-F substrates. However, on HA-F a higher number of clusters were observed. Large double actin rings with some podosomes, i.e. small actin dots, were seen for OCP on sin-HA, and very large (diameter: 60-250 μm) osteoclasts with double actin rings and podosome belt, were seen on TCPS used as a control surface (Fig. 2).

On HA-C and HA-F different cell arrangements were seen by SEM (Fig. 3). OCP were able to attach on the surface of HA-C with a flat appearance (Fig. 3a), as they spread on the rough surface, showing many dorsal microvilli and connecting each other (Fig. 3b).

Under the cell bodies no evident differences in HA-C microstructure were observed that could be associated with material resorption by the cells (Fig. 3c).

On HA-F a high number of OCP was seen over the material surface, with elongated morphology and evident nuclei, as well as cell-cell connecting filopodia (Fig. 3 d,e). Looking at the material under the cell bodies, no clear changes in the underlying typical needle-like microstructure were seen (Fig. 3f).

On sin-HA (reference material), many osteoclasts with spread and flattened morphology were formed, and active resorption pits, clearly distinguishable from the intrinsic porosity of the material, were seen on the sin-HA surface (Fig. 4a,b). Under such pits the material microstructure was changed, with typical signals of acidic degradation (Fig. 4c).

Ultrastructural observation using SEM showed that on TCPS many osteoclasts were formed by fusion of OCP and displayed the typical aspect, i.e. large cells with a rough membrane (Fig. 4 d,e,f). Osteoclasts were tightly attached to this surface, with cellular filopodia connecting adjacent osteoclast to get a network. Also, clusters of non fused OCP were observed.

3.2.2 OC recognition

Tartrate-resistant acid phosphatase (TRAP) staining and Hoechst 33258 dye for nuclei, i.e. typical markers of osteoclasts, were used to characterize the cells after 21 days in differentiating medium on the different surfaces. All the surfaces were densely populated by TRAP-positive red cells, with sin-HA and HA-F scoring the higher number of OCP (Fig. 5).

The release of TRAP5b, an active enzyme degrading bone matrix proteins, is considered a specific marker of late osteoclast differentiation. Following enzymatic assay in the culture supernatants, TRAP5b was consistently released by OCP on HA-C and HA-F, as well as on sin-HA and TCPS (Fig. 6) with no statistically significant differences between them. After 21 days of culture in osteoclast differentiation medium the gene expression of CTSK, MMP-9 and v-ATPase was analyzed by Real-time PCR, with data normalized to the rRNA 18s control housekeeping gene.

Gene expression by OCP at 21 days was compared to 'day 0', i.e. to gene expression of PBMC before seeding on the surfaces and differentiation induction.

CTSK was consistently expressed only by OCP on TCPS. Instead, a significant increase in MMP-9 gene expression was observed on day 21 in all the cultures, with a higher expression on HA-C than on HA-F. The highest expression of MMP-9 was recorded on TCPS. V-ATPase was already expressed at day 0, with an increase on day 21 against day 0 only for OCP on TCPS (Fig. 7).

3.2.3 Ionic fluctuations in the cell culture medium

The changes of calcium (Ca^{++}) and phosphorus (P^{5+}) in the culture medium in contact with HA-C, HA-F and sin-HA substrates with and without cells is shown in Fig. 8. In sin-HA, no changes in calcium and phosphorus concentration were observed compared to the TCPS control. In contrast, biomimetic HA-C and HA-F showed a depletion of calcium and an increased concentration of phosphorus, being the changes more pronounced for the HA-F than for the HA-C. Calcium concentration was higher for all samples with cells compared to the samples without cells. The variation in the calcium concentration tended to decrease along the experimental time.

3.3 Indirect-contact assay

Each material extract supplemented with 25% of RANKL-containing osteoblast supernatant was added to the cell cultures every 3 days. Osteoclast differentiation was assessed using TRAP staining at 14 days and gene expression at 21 days. Significance of the gene expression data was calculated against day 0, i.e. at seeding of PBMC.

OCP challenged with HA-C extract differentiated to osteoclasts similarly to cells cultured with differentiating medium only on TCPS (control) and with sin-HA extract. Some osteoclasts were seen in the culture challenged with the HA-F extract, too (Fig. 9).

As shown in Fig. 10, OCP challenged with HA-C or HA-F extracts expressed CTSK at 21 days, even if less than sintered-HA and TCPS, and significantly more than at time 0. MMP-9 and v-ATPase, were highly expressed by OCP on sin-HA and TCPS. These genes were recorded also for HA-C treated cells, with a value similar to those expressed at time 0. HA-F treated cells had a lower expression of MMP-9 and v-ATPase in comparison to time 0.

4. DISCUSSION

Most of the literature on *in vitro* calcium phosphate (CaP) materials compatibility deals with osteoblasts or osteoblast-like cells, as their adhesion, proliferation and function on these materials are taken as proofs of good bone integration [4, 17, 18]. However, a balance between osteoblastic and osteoclastic activities is required for a successful biomaterial therapy, as bone substitutes have to be resorbed with time and replaced by new bone deposited by osteoblasts. The coupling of bone formation to resorption, already suggested 30 years ago by the group of Baylink [19], is increasingly recognized as a complex dynamic process: osteoclasts produce many molecules affecting osteoblasts and vice-versa [20-22].

The release of pro-osteogenic signals coming from osteoclasts has been recently confirmed to occur also on CaP substrates [23-24]. Therefore, the attachment and activity of osteoclasts on CaP surfaces has to be seen not only for their resorptive function, but also as an essential preparatory step to substrate replacement by new bone [25].

This study was aimed at verifying if blood-derived human OCP may differentiate to osteoclasts and resorb the substrate when plated on HA disks with different microstructures. Also, direct and indirect contact assays were performed to discern the effects on osteoclast formation of 1) surface-cell interaction and 2) ion exchange potentially occurring at the HA/cell culture medium interphase. In both assays, osteoclast maturation was induced by osteoblast-derived differentiating medium.

HA disks were prepared by a low temperature setting reaction, resulting in a more biomimetic composition, topography and crystal size than sintered HA, prepared by typical solid state reaction at high temperature.

Using the direct contact system, we found that after 21 days of culture osteoclast-like cells were formed on all the surfaces, but their density, morphology and potential resorbing activity were different.

On the control and reference surfaces, TCPS and sin-HA respectively, osteoclasts were formed, as shown by large, continuous actin rings at the cell periphery as seen by confocal microscopy (Fig. 2), as well as by a large size, a flattened aspect and the cell-cell connections seen by SEM (Figs. 3 and 4). Moreover, pits due to active resorption by osteoclasts were seen on sin-HA, with some aspects of acidic degradation of the material under the cells (Fig. 4). The differentiation of precursors to osteoclasts on TCPS and sin-HA was confirmed by the TRAP positive staining of multinucleated cells, as well as by the release of active TRAP5b enzyme in the medium. Furthermore, gene analysis showed a high expression of CTSK, MMP-9 and v-ATPase at 21 days

from seeding on TCPS, whereas on sin-HA only MMP-9 was consistently overexpressed compared to time 0. All together, these findings confirmed that the protocol adopted to induce OCP differentiation to mature osteoclasts was effective.

On HA-C substrate OCP attached using actin-rich podosomes, but due to surface irregularities, a complete actin ring was absent. By SEM, the cells were flattened on the surface, similar to cells on sin-HA, and used filopodia to contact other cells and to attach to the irregular surface. Also, the cell surface rich in microvilli suggested an intense cell activity. TRAP positivity and multinuclearity of cells on HA-C, as well as TRAP5b release, confirmed that osteoclasts differentiated on the surface, even if less in number compared to sin-HA. According to gene expression data, only MMP-9 was consistently overexpressed by osteoclasts on HA-C compared to day 0.

After 21 days of culture on HA-F substrate a very high number of OCP attached using actin-rich podosomes, likely due to the needle-like microstructure of the surface. By SEM it was observed that the HA-F samples were covered by many spindle-shaped cells which connected each other. TRAP and nuclei staining also showed a high density of cells with an elongated morphology, with only a few osteoclast-like cells. Despite the large number of attached cells, the low gene expression levels confirmed the paucity of mature osteoclasts seen with TRAP staining.

Using the indirect contact assay, we found that HA-C-treated OCP generated mature osteoclasts and expressed CTSK, MMP-9 and ν -ATPase genes, following the same trend than sin-HA-treated OCPs, even if with a lower expression level. Less differentiated osteoclasts were seen in the cultures treated with HA-F extract, which also scored the lowest osteoclast gene expression.

It is known that one of the main surface features affecting cell attachment is topography, as shown in a number of studies, and a certain degree of roughness has been shown to positively affect osteoblasts [26] and osteoclasts [27] adhesion and/or differentiation.

Likewise, our results show that the cell-cell fusion, required for osteoclast formation, as well as the formation of a good sealing ring to resorb the substrate, are strongly affected by the material topography.

In our study, the chemistry of the two biomimetic HA substrates is equivalent. In contrast, surface topography is clearly different, with HA-F having a smaller roughness and a higher SSA than HA-C, and both having a different topography compared to sin-HA used as a reference.

These features have been shown to affect protein adsorption onto the surface [12], and also the response of osteoblast-like cells [13]. Therefore, it is likely that also osteoclast differentiation and activity is modulated by these parameters, even if osteoclasts show a certain degree of 'rugophilia' [28].

Although a number of results of our study point at the differentiation of OCP to osteoclasts on the biomimetic HA surface, they are less in number and with different morphology compared to mature osteoclasts developed on sin-HA or TCPS.

This is not surprising, as osteoclast formation is the result of a high density of confluent OCP which fuse together [29, 30]. We suggest that the inability to migrate, fuse and form a stable actin ring (and a sealing zone), due to the plate- and needle-shaped microstructure of HA-C and HA-F surfaces, would prevent osteoclast-like cells to become mature osteoclasts driving consistent signals of resorption.

In our hands, podosome formation was observed on both the biomimetic HA surfaces, but these structures do not further fuse to form large typical actin rings.

As discussed by Costa-Rodrigues *et al.*, even if it has been shown that rougher surfaces can support a high degree of osteoclast development when it is mediated by soluble factors (as in our study), material steric hindrance might become a problem for cell-to-cell interactions, and, noticeably, for cell fusion [28]. In another study an inverse linear correlation between the number of actively resorbing osteoclasts with surface microporosity of β -TCP was demonstrated, but rabbit Oc and not human PBMC were tested in such a study [31]. That coarse or highly irregular surfaces may hinder osteoclast attachment and/or differentiation, while surfaces with a 'low' roughness allow both processes, has been confirmed by other studies. Using human PBMC cultured on carbonated hydroxyapatite (CA), hydroxyapatite (HA) and b-tricalcium phosphate (TCP) with similar roughness, i.e. $R_a = 0.5\text{--}0.6\ \mu\text{m}$, osteoclasts were shown to adhere and differentiate into giant multinuclear TRAP-positive cells on every type of surface, even if with more 'mature OC on CA [32]. Davison [23] showed that the survival, differentiation, and resorbing function of human osteoclasts was promoted on beta-tricalcium phosphate (TCP) with a low surface roughness, i.e. $R_a = 0.158\ \mu\text{m}$, while TCP with $R_a = 1.597\ \mu\text{m}$ impeded OC survival and resorption. Accordingly, in another study 'a disrupted F-actin organization, with individual podosomes, and podosome clusters and belts along the cell periphery', as well as 'less TRAP-positive staining on HA surfaces with increased levels of complexity and roughness' were displayed by osteoclasts on 2 μm -rough HA surfaces [33]. Moreover, surface irregularities at the micrometer scale may hamper the formation of a sealing zone, too, by interrupting the OC matrix adhesiveness [34].

Human osteoclast precursor cells are sensitive to nano-structures, too: when cultured on three topographically different hydroxyapatites, OC have been shown to react differently to micro- vs nano-structured HA surfaces, the latter appearing less attractive to osteoclastic differentiation and function, compared to a micro-sized grain topography [35].

Therefore, focusing on human osteoclast precursors only, apparently their adhesion and differentiation preferentially occur on CaP-based substrates with a ‘moderate’ surface roughness at the microscale.

Other material and surface features do affect osteoclast formation and activity.

A significant correlation between initial material-dependent changes in the pH of culture supernatants and material resorbability, with effects on osteoclast multinuclearity and material resorption has been demonstrated by Keller *et al.* [8].

Since osteoclasts have also been recognized as ‘mechanosensitive’ cells, which are able to sense rigidity of the substrate, a different stiffness of the substrates may regulate osteoclastogenesis [36], and also resorbability, as shown by Kruppke [25], plays a major role in OC response *in vitro*.

In our study, the surface pre-conditioning with medium prior to cell seeding prevented initial excessive pH changes, and the stiffness of the substrates was not assessed.

As a matter of fact, the variety of osteoclast type, CaP composition, submicro- and micro-structure, physical parameters and *in vitro* models hinder a comprehensive and definitive understanding of the osteoclast/material interaction [37].

We suggest that in our system on biomimetic HA surfaces a number of mononuclear cells fused together to form osteoclast-like cells, but final maturation to functional osteoclasts was not always reached due to topographical reasons, that is podosome fusion to organized actin ring and sealing zone formation were hampered by the irregular surface structure. A similar mechanism was described by Addadi *et al.*, who observed that ‘the assembly of the basic adhesion unit (i.e. the podosome) in osteoclasts is intrinsically regulated, irrespective of the particular adhesive surface used. However, further development of podosomal super-structures is surface-sensitive’ [38].

Indeed, this ‘irregular’ osteoclast morphology may in turn cause the low resorption activity recorded in our study. Moreover, the finding of osteoclast-like cells on biomimetic HA surfaces does not necessarily imply that they are active. The inability to seal a zone to be resorbed may explain the absence of evident resorption pits on the biomimetic HA, while this was seen on sintered-HA. According to Geblinger D. *et al.* on bone ‘the resorption lacuna must be well defined and sufficiently stable over time to allow resorption to occur’ [39]: this is rather unlikely to occur on our microstructured biomimetic surfaces, while on sin-HA the surface allowed for OCP fusion and resorptive activity with pit formation.

It is interesting to note, regarding the finding of no clear resorptive activity for HA-C and HA-F, that osteoclasts, irrespective of their bone resorption activity, are able to produce bone anabolic signals to osteoblasts [40]. Therefore, it cannot be excluded that the different populations of

osteoclasts, resorbing and non-resorbing ones, present on biomimetic HA materials could cooperate with osteoblasts to trigger new bone formation.

Of note is also the depletion of calcium and the release of phosphate in the culture medium produced by biomimetic HA, as revealed by ICPS-OES measurements (Fig. 8): this finding has already been shown in previous papers [13, 41,42] and is related to the calcium deficiency and high SSA of the biomimetic HA. In a previous work [41] we investigated the ionic reactivity of biomimetic HA in DMEM, finding also an uptake of calcium and a release of phosphate. The uptake of calcium can be associated to the maturation process of the calcium deficient biomimetic HA ($\text{Ca}_9(\text{PO}_4)_5(\text{HPO}_4)\text{OH}$, with Ca/P molar ratio 1.5), to stoichiometric HA ($\text{Ca}_{10}(\text{PO}_4)_6(\text{OH})_2$, with Ca/P molar ratio 1.67) that is more thermodynamically stable [43,44]. The release of phosphate can be attributed to the replacement of phosphate ions with other ions available in the cell culture medium, typically carbonate, as proven by the presence of carbonate bands in the FTIR spectra of biomimetic-HA samples after immersion in DMEM [41]. This ion exchange process is amplified by the high SSA of the biomimetic materials, as well as by the presence of non-apatitic domains on the crystal surface of nanoapatites, giving them a higher reactivity than that of sintered HA [43,44]. Sin-HA, which is stoichiometric and has a lower SSA, did not induce variation in the ionic composition of the cell culture medium. In the presence of cells, higher levels of calcium were recorded in the cell culture medium, which could be caused by a reduction of the surface exposed, which is able to uptake calcium from the medium in the case of biomimetic HA. Furthermore, the differences in SSA between HA-C and HA-F produced differences in the extent of ionic exchanges. In our hands HA-F, with higher SSA, was subtracting more calcium from the microenvironment than HA-C. This could be an additional potential reason for the different behaviour of the two biomimetic HA regarding osteoclast formation and activity.

Concerning the gene expression results, in the direct contact assay MMP-9 was expressed by OCP on all the HA surfaces, while no CTSK and v-ATPase expression was found (compared to day 0). This did not happen for osteoclasts on TCPS, which had a regular morphology, with evident TRAP staining and a lot of nuclei, and high expression in comparison to day 0 of CTSK, MMP-9 and v-ATPase, that are all the features shared by mature osteoclasts. Comparing HA-C and HA-F in both systems (direct and indirect), apparently gene expression for HA-C is always higher than with HA-F. We hypothesize that the lower calcium concentration in the HA-F culture systems compared to HA-C could have differentially regulated gene expression and osteoclast formation. This may be supported by the gene expression results with extracts, where CTSK, MMP-9 and v-ATPase were expressed by OCP on sin-HA and TCPS, where no change in calcium concentration was recorded, with often higher expression in sin-HA than TCPS.

It is known that calcium ions (Ca^{++}) affect osteoclast differentiation and function. Osteoclasts and their progenitors show a cell membrane calcium receptor [45], and intracellular calcium is tightly regulated by calcium entry from the extracellular fluid, and a mechanism involving Ca^{++} and calcineurin leads to osteoclast differentiation [46,47]. Also, extracellular calcium concentration has been found to signal for osteoclasts survival and differentiation by modulation of the cytosolic Ca^{++} levels [48,49], but the role of calcium signaling in osteoclasts is still under intense study [50,51]. As reported by the group of Brandi, on the active bone surfaces only modest and gradual changes of Ca^{2+} , ranging from 0.5 mM during formation to ≥ 2 mM during resorption, occur, and these values are very close to the calcium oscillations detected in our study by ICP-OES in the direct contact assay [45]. Therefore, we do not expect a major effect of calcium on the behaviour of osteoclasts in our protocol.

The effect of phosphate on osteoclasts is nearly unknown. An *in vivo* study on phosphate metabolism in ADP P2Y13 receptor-knockout mice demonstrated that young mice with 16 % higher serum phosphorous level compared to mature mice had 73 % fewer osteoclasts [52]. Furthermore, it was observed that soluble inorganic polyphosphates prevent the differentiation of OCP to the mature osteoclasts by inhibiting the phosphorylation of the $\text{I}\kappa\text{B}\alpha$ kinase and the expression of TRAP [53], and extracellular inorganic phosphate dose-dependently reduced RANKL-induced osteoclastic differentiation of monocyte precursors [54].

The results of this study improve our understanding of the fundamental mechanisms involved in osteoclastic differentiation mediated by calcium phosphate materials.

We showed that the *in situ* differentiation of OCP into osteoclasts points at a major role of topography, which in turn influences ionic exchange, as higher ionic fluctuations are produced in materials with larger SSA.

In static culture systems, any ionic fluctuation can markedly influence cell response, making it difficult to translate the results to the *in vivo* scenario, where fluid circulation buffers ionic fluctuations. Moreover, it has to be considered that when cells are cultured directly on the material they will sense the local concentration in the close vicinity of the surface, which is probably different from the average ionic concentrations measured in the cell culture medium and found in the extracts. This adds a degree of complexity in the interpretation of the results.

In our system we found that the materials with rougher surface topography, which in turn results in calcium depletion from the medium, may hamper osteoclast formation *in vitro*, leading to a lower *in vitro* degradation of the biomimetic HA substrates (HA-C and HA-F). This is apparently in contrast with the fact that, due to their calcium deficiency and small crystal size, they are more soluble than crystalline stoichiometric HA, and indeed faster resorption *in vivo* has been

demonstrated [55]. Additionally, in previous works we have demonstrated that bone formation elicited by biomimetic HA biomaterials is preceded by osteoclastic resorption, which leads to a synchronized timing of bone formation and material degradation [55,56].

This is just another example of the need to be cautious when translating *in vitro* results to the *in vivo* performance, where many other factors come into play [57,58].

Indeed, the *in vivo* complexity of the osteoblast-osteoclast interaction on surfaces, in terms of timing, intensity, signal recognition, receptor activation, molecular pathways, not to mention microenvironmental pH, ion oscillations and interactions with other cells, are hard to simulate *in vitro*. Nonetheless, the *in vitro* culture protocols provide informative responses and OB-OC co-culture are a good model to study the bi-directional cooperation of osteoclasts and osteoblasts. That osteoclast-osteoblast paracrine signaling is a crucial part of the bone remodeling process and should not be hindered in the treatment of bone diseases is a largely accepted concept [59], and this increasing knowledge should be taken into account when testing new drugs known to affect bone coupling or designing tissue engineering strategies for bone [37].

5. CONCLUSION

This *in vitro* study investigated osteoclast formation from human blood-derived osteoclast precursors induced to differentiate after seeding on HA materials with different surface structure or after challenge with their extracts.

In our experimental system the biomimetic HA-C and HA-F materials, with rough and porous surfaces and high SSA were permissive surfaces for OCP attachment and survival. Subsequent fusion and resorptive activity were partially hampered by surface micro- and nano-structure. Nonetheless, osteoclast-like cells and osteoclasts were able to differentiate from peripheral blood mononuclear cells onto calcium phosphates in 3 weeks, showing TRAP activity, even if no evidence of resorption activity was found. In contrast, the smoother and less reactive surface of sin-HA better allowed osteoclast formation and activity, producing clear resorption pits on the surface. The comparison between direct and indirect cultures suggests that OCP are not only sensitive to topography, but also to the ionic exchanges in the surrounding medium.

In conclusion, a comprehensive understanding of the physiological effect and micro-environmental changes derived from CaP engraftment in bone, including bioactivities along with biocompatibility, is mandatory in considering potential usage in patients.

Acknowledgments

This research was funded by the Italian Ministry of Health, Ricerca Corrente, project ‘Strategie di rigenerazione ossea: dall’interazione materiale/cellule dell’osso ai markers riparativi’ (2013-2016), and the Spanish Government, project MINECO MAT2015-65601, co-funded by the EU through ERDF. MPG acknowledges the ICREA Academia award by the Generalitat de Catalunya.

REFERENCES

1. P.R. Jensen, T.L. Andersen, B.L. Pennypacker, L.T. Duong, L.H. Engelholm, J.M. Delaissé, A supra-cellular model for coupling of bone resorption to formation during remodeling: lessons from two bone resorption inhibitors affecting bone formation differently, *Biochem. Biophys. Res. Comm.* 443 (2014) 694–699.
2. T.J. Martin, N.A. Sims, Coupling the activities of bone formation and resorption: a multitude of signals within the basic multicellular unit, *BoneKEY Reports* 3 (2014) Article number: 481.
3. S.A. Redey, S. Razzouk, C. Rey, D. Bernache-Assollant, G. Leroy, M. Nardin, G. Cournot, Osteoclast adhesion and activity on synthetic hydroxyapatite, carbonated hydroxyapatite, and natural calcium carbonate: Relationship to surface energies, *J. Biomed. Mater. Res.* 45 (1999) 140–147.
4. S. Samavedi, A.R. Whittington, A.S. Goldstein, Review, Calcium phosphate ceramics in bone tissue engineering: A review of properties and their influence on cell behavior, *Acta Biomaterialia* 9 (2013) 8037–8045.
5. K.A. Gross, D. Muller, H. Lucas, D.R. Haynes, Osteoclast resorption of thermal spray hydroxyapatite coatings is influenced by surface topography, *Acta Biomaterialia* 8 (2012) 1948–1956.
6. J. Choy, C.E. Albers, K.A. Siebenrock, S. Dolder, W. Hofstetter, F.M. Klenke, Incorporation of RANKL promotes osteoclast formation and osteoclast activity on β -TCP ceramics, *Bone* 69 (2014) 80–88.
7. A. Konermann, M. Staubwasser, C. Dirk, L. Keilig, C. Bourauel, W. Götz, A. Jäger, C. Reichert, Bone substitute material composition and morphology differentially modulate calcium and phosphate release through osteoclast-like cells, *Int. J. Oral. Maxillofac. Surg.* 43 (2014) 514–521.
8. J. Keller, S. Brink, B. Busse, A.F. Schilling, T. Schinke, M. Amling, T. Lange, Divergent resorbability and effects on osteoclast formation of commonly used bone substitutes in a human in vitro-assay, *PLoS One.* 7 (2012) e46757.
9. A. Bernhardt, M. Schumacher, M. Gelinsky, Formation of osteoclasts on calcium phosphate bone cements and polystyrene depends on monocyte isolation conditions, *Tissue Eng. Part C Methods.* 21 (2015) 160–170.

10. M.P. Ginebra, E. Fernandez, E.A. De Maeyer, R.M. Verbeeck, M.G. Boltong, J. Ginebra, F.C. Driessens, J.A. Planell, Setting reaction and hardening of an apatitic calcium phosphate cemen, *J. Dent. Res.* 76 (1997) 905-912.
11. M.P. Ginebra, F.C. Driessens, J.A. Planell, Effect of the particle size on the micro and nanostructural features of a calcium phosphate cement: a kinetic analysis, *Biomaterials* 25 (2004) 3453-3462.
12. C. M. Espanol, R.A. Perez, E.B. Montufar, C. Marichal, A. Sacco, M.P. Ginebra, Intrinsic porosity of calcium phosphate cements and its significance for drug delivery and tissue engineering applications, *Acta Biomaterialia* 5 (2009) 2752–2762.
13. E. Engel, S. Del Valle, C. Aparicio, G. Altankov, L. Asin, J.A Planell, M.P Ginebra, Discerning the role of topography and ion exchange in cell response of bioactive tissue engineering scaffolds, *Tissue Engineering A* 8 (2008) 1341-1351.
14. M.E. Abdelgawad, J.M. Delaisse, M. Hinge, P.R. Jensen, R.W. Alnaimi, L. Rolighed, L.H. Engelholm, N. Marcussen, T.L. Andersen, Early reversal cells in adult human bone remodeling: osteoblastic nature, catabolic functions and interactions with osteoclasts, *Histochem. Cell Biol.* 145 (2016) 603-615.
15. D. Granchi, I. Amato, L. Battistelli, G. Ciapetti, S. Pagani, S. Avnet, N. Baldini, A. Giunti, Molecular basis of osteoclastogenesis induced by osteoblasts exposed to wear particles, *Biomaterials* 26 (2005) 2371-2379.
16. S. Avnet, R. Pallotta, F. Perut, N. Baldini, M.G. Pittis, A. Saponari, E. Lucarelli, B. Dozza, T. Greggi, N.M. Maraldi, C. Capanni, E. Mattioli, M. Columbaro, G. Lattanzi, Osteoblasts from a mandibuloacral dysplasia patient induce human blood precursors to differentiate into active osteoclasts, *Biochim Biophys Acta* 1812 (2011) 711-718.
17. J. Zhang, X. Luo, D. Barbieri, A.M.C. Barradas, J.D. de Bruijn, C.A. van Blitterswijk, H. Yuan, The size of surface microstructures as an osteogenic factor in calcium phosphate ceramics, *Acta Biomaterialia* 10 (2014) 3254-3263.
18. Y.C. Chai, A. Carlier, J. Bolander, S.J. Roberts, L. Geris, J. Schrooten, H. Van Oosterwyck, F.P. Luyten, Current views on calcium phosphate osteogenicity and the translation into effective bone regeneration strategies, *Acta Biomater.* 8 (2012) 3876-3887.
19. G.A. Howard, B.L. Bottemiller, R.T. Turner, J.I. Rader, D.J. Baylink, Parathyroid hormone stimulates bone formation and resorption in organ culture: evidence for a coupling mechanism, *Proc Natl Acad Sci USA* 78 (1981) 3204–3208.
20. H.H. Lu, S.D. Subramony, M.K. Boushell, X. Zhang, Tissue engineering strategies for the regeneration of orthopedic interfaces, *Ann. Biomed. Eng.* 3 (2010) 2142–2154.
21. K. Henriksen, M.A. Karsdal, T.J. Martin, Osteoclast-Derived Coupling Factors in Bone Remodeling, *Calcif. Tissue Int.* 94 (2014) 88-97.
22. N.A. Sims, T.J. Martin, Coupling Signals between the Osteoclast and Osteoblast: How are Messages Transmitted between These Temporary Visitors to the Bone Surface?, *Front. Endocrinol. (Lausanne)* 6 (2015) 41.
23. N.L. Davison, B. ten Harkel, T. Schoenmaker, X. Luo, H. Yuan, V. Everts, F. Barrère-de Groot, J.D. de Bruijn, Osteoclast resorption of beta-tricalcium phosphate controlled by surface architecture, *Biomaterials* 35 (2014) 7441-7451.
24. N.L. Davison, J. Su, H. Yuan, J.J. van den Beucken, J.D. de Bruijn, F. Barrère-de Groot, Influence of surface microstructure and chemistry on osteoinduction and osteoclastogenesis by biphasic calcium phosphate discs, *Eur. Cell Mater.* 29 (2015) 314-329.

25. B. Kruppke, J Farack, A.S. Wagner, S. Beckmann, C. Heinemann, K. Glenske, S. Rößler, H.P. Wiesmann, S. Wenisch, T. Hanke, Gelatine modified monetite as a bone substitute material: An in vitro assessment of bone biocompatibility, *Acta Biomater.* 32 (2016) 275-285.
26. B.D. Boyan, S. Lossdörfer, L. Wang, G. Zhao, C.H. Lohmann, D.L. Cochran, Z. Schwartz, Osteoblasts generate an osteogenic microenvironment when grown on surfaces with rough microtopographies, *Eur. Cell Mater.* 24 (2003) 22-27.
27. T. Matsunaga, H. Inoue, T. Kojo, K. Hatano, T. Tsujisawa, C. Uchiyama, Y. Uchida, Disaggregated osteoclasts increase in resorption activity in response to roughness of bone surface, *J Biomed Mater Res.* 48 (1999) 417-423.
28. J. Costa-Rodrigues, A. Fernandes, M.A. Lopes, M.H. Fernandes, Hydroxyapatite surface roughness: Complex modulation of the osteoclastogenesis of human precursor cells, *Acta Biomater.* 8 (2012)1137–1145.
29. M. Motiur Rahman, S. Takeshita, K. Matsuoka, K. Kaneko, Y. Naoe, A. Sakaue-Sawano, A. Miyawaki, K. Ikeda, Proliferation-coupled osteoclast differentiation by RANKL: Cell density as a determinant of osteoclast formation, *Bone* 81 (2015) 392-399.
30. A.S. Hobolt-Pedersen, J.M. Delaissé, K. Søre, Osteoclast fusion is based on heterogeneity between fusion partners, *Calcif. Tissue Int.* 95 (2014) 73-82.
31. G. Zimmer, A. Rohrhofer, K. Lewis, A. Goessl, O. Hoffmann, The surface microporosity of ceramic biomaterials influences the resorption capacity of osteoclasts, *J. Biomed. Mater. Res. A* 101 (2013) 3365-3371.
32. M. Nakamura, T. Hentunen, J. Salonen, A. Nagai, K. Yamashita, Characterization of bone mineral resembling biomaterials for optimizing human osteoclast differentiation and resorption, *J Biomed Mater Res Part A* 101A (2013) 3141–3151.
33. D.O. Costa, P.D.H. Prowse, T. Chrones, S.M. Sims, D.W. Hamilton, A.S. Rizkalla, S.J. Dixon, The differential regulation of osteoblast and osteoclast activity by surface topography of hydroxyapatite coatings, *Biomaterials* 34 (2013) 7215-7226.
34. F. Anderegg, D. Geblinger, P. Horvath, M. Charnley, M. Textor, L. Addadi, B. Geiger, Substrate Adhesion Regulates Sealing Zone Architecture and Dynamics in Cultured Osteoclasts, *PLoS ONE* 6 (2011) e28583.
35. J. Costa-Rodrigues, S. Carmo, I.P. Perpétuo, F.J. Monteiro, M.H. Fernandes, Osteoclastogenic differentiation of human precursor cells over micro- and nanostructured hydroxyapatite topography, *Biochim. Biophys. Acta* 1860 (2016) 825–883.
36. K. Pernelle, L. Imbert, C. Bossier, J.C. Auregan, M. Cruel, A. Ogier, P. Jurdic, T. Hoc, Microscale mechanical and mineral heterogeneity of human cortical bone governs osteoclast activity, *Bone* 94 (2016) 42-49.
37. R. Detsch, A.R. Boccaccini, The role of osteoclasts in bone tissue engineering, *J Tissue Eng Regen Med.* 9 (2015) 1133-1149.
38. D. Geblinger, B. Geiger, L. Addadi, Surface-induced regulation of podosome organization and dynamics in cultured osteoclasts, *Chembiochem.* 10 (2009) 158-165.
39. D. Geblinger, C. Zink, N.D. Spencer, L. Addadi, B. Geiger, Effects of surface microtopography on the assembly of the osteoclast resorption apparatus, *J. R. Soc. Interface* 9 (2012) 1599–1608.

40. K. Henriksen, K.V. Andreassen, C.S. Thudium, K.N.S. Gudmann, I. Moscatelli, C.E. Crüger-Hansen, A.S. Schulz, M.H. Dziegiel, J. Richter, M.A. Karsdal, A.V. Neutzky-Wulff, A specific subtype of osteoclasts secretes factors inducing nodule formation by osteoblasts, *Bone* 51 (2012) 353–361.
41. J. Gustavsson, M.P. Ginebra, E. Engel, J. Planell, Ion reactivity of calcium-deficient hydroxyapatite in standard cell culture media, *Acta Biomaterialia* 7 (2011) 4242–4252.
42. J. Gustavsson, M.P. Ginebra, J. Planell, E. Engel, Osteoblast-like cellular response to dynamic changes in the ionic extracellular environment produced by calcium-deficient hydroxyapatite, *J. Mater. Sci. Mater. Med.* 23 (2012) 2509–2520.
43. S. Cazalbou, D. Eichert, X. Ranz, C. Drouet, C. Combes, M.F. Harmand, C. Rey, Ionic exchanges in apatites for biomedical applications, *J. Mater. Sci. Mater. Med.* 16 (2005) 405–409.
44. S. Cazalbou, C. Combes, D. Eichert, C. Rey, Adaptative physico-chemistry of bio-related calcium phosphates, *J. Mater. Chem.* 14 (2004) 2148–2153.
45. L. Cianferotti, A.R. Gomes, S. Fabbri, A. Tanini, M.L. Brandi, The calcium-sensing receptor in bone metabolism: from bench to bedside and back, *Osteoporos Int.* 26 (2015) 2055–2071.
46. T. Negishi-Koga, H. Takayanagi, Ca²⁺-NFATc1 signaling is an essential axis of osteoclast differentiation, *Immunol. Rev.* 231 (2009) 241–256.
47. H. Zhao, X. Liu, H. Zou, N. Dai, L. Yao, Q. Gao, W. Liu, J. Gu, Y. Yuan, J. Bian, Z. Liu, Osteoprotegerin induces podosome disassembly in osteoclasts through calcium, ERK, and p38 MAPK signaling pathways, *Cytokine* 71 (2015) 199–206.
48. M. Zaidi, B.S. Moonga, C.L. Huang, Calcium sensing and cell signaling processes in the local regulation of osteoclastic bone resorption, *Biol. Rev.* 79 (2004) 79–100.
49. A. Del Fattore, A. Teti, N. Rucci, Osteoclast receptors and signaling, *Arch. Biochem. Biophys.* 473 (2008) 147–160.
50. S.Y. Hwang, J.W. Jr. Putney, Calcium signaling in osteoclasts, *Biochim. Biophys. Acta (BBA) – Mol Cell Res.* 1813 (2011) 979–983.
51. H. Kajiya, Calcium signaling in osteoclast differentiation and bone resorption, *Adv Exp Med Biol.* 740 (2012) 917–932.
52. N. Wang, B. Robaye, F. Gossiel, J.M. Boeynaems, A. Gartland, The P2Y₁₃ receptor regulates phosphate metabolism and FGF-23 secretion with effects on skeletal development, *FASEB J.* 28 (2014) 2249–2259.
53. X.H. Wang, H.C. Schröder, B. Diehl-Seifert, K. Kropf, U. Schloßmacher, M. Wiens, W.E.G. Müller, Dual effect of inorganic polymeric phosphate/polyphosphate on osteoblasts and osteoclasts in vitro, *J Tissue Eng Regen Med.* 7 (2013) 767–776.
54. A. Mozar, N. Haren, M. Chasseraud, L. Louvet, C. Mazière, A. Wattel, R. Mentaverri, P. Morlière, S. Kamel, M. Brazier, J.C. Mazière, Z.A. Massy, High extracellular inorganic phosphate concentration inhibits RANK-RANKL signaling in osteoclast-like cells, *J Cell Physiol.* 215 (2008) 47–54.
55. A. Kovtun, M.J. Goeckelmann, A.A. Niclas, E.B. Montufar, M.P. Ginebra, J.A. Planell, M. Santin, A. Ignatius, In vivo performance of novel soybean/gelatin-based bioactive and injectable hydroxyapatite foams, *Acta Biomaterialia* 12 (2015) 242–249.

56. E. Cuzmar, R.A. Perez, M.C. Manzanares, M.P. Ginebra, J. Franch, In vivo osteogenic potential of biomimetic hydroxyapatite/collagen microspheres: comparison with injectable cement pastes, PLoS ONE 10 (2015) e0131188.
57. J.X. Lu, A. Gallur, B. Flautre, K. Anselme, M. Descamps, B. Thierry, P. Hardouin, Comparative study of tissue reactions to calcium phosphate ceramics among cancellous, cortical, and medullar bone sites in rabbits, J. Biomed. Mater. Res. 42 (1998) 357–367.
58. D. Heymann, G. Pradal, M. Benahamed, Cellular mechanisms of calcium phosphate ceramic degradation, Hist. Histopathol. 14 (1999) 871-877.
59. Y. Shiwaku, L. Neff, K. Nagano, K.I. Takeyama, J. de Bruijn, M. Dard, F. Gori, R. Baron, The Crosstalk between Osteoclasts and Osteoblasts Is Dependent upon the Composition and Structure of Biphasic Calcium Phosphates, PLOS ONE 10 (2015) e0132903.

CAPTIONS

Fig. 1 Scanning electron micrographs and optical interferometry images of HA-C (a-c), HA-F (d-f) and sintered-HA (g-i), showing the microstructure and surface topography of the samples.

Fig. 2: Rhodamine-phalloidin staining of actin in OCP cultured for 21 days in direct contact with HA substrates and TCPS. Small actin dots are indicated by arrowheads (a: HA-C; b: HA-F; c: sin-HA; d: TCPS, scale bar= 20 micrometers).

Fig. 3 Scanning electron micrographs showing the morphology of OCP cultured on biomimetic HA-C (a,b,c) and HA-F (d,e,f). Top row: spread and flattened cells (arrows) with connections between them and some fusion (a,b). FIB cut showing the HA-C microstructure below a representative cell (c). Bottom row: spindle-shaped cells with evident nuclei (arrows) and filopodia connections between them (a, b). FIB cut showing the HA-F microstructure below a representative cell (c).

Fig. 4. Scanning electron micrographs showing the morphology of osteoclasts formed on sin-HA (a,b,c) and TCPS (d,e,f). Top row: (a) spread and flattened osteoclasts (arrowheads) together with two resorption pits (yellow arrows) and three pores typical of sintered materials (+); (b) FIB cut showing the sin-HA microstructure below a representative osteoclast (osteoclast edges are marked by a red line); (c) Boundary between the pit produced by osteoclast and the original sin-HA surface (area within the square in a). Original sin-HA structure is indicated by * and the degraded material is indicated by arrows. Bottom row: on TCPS fused OCP form large osteoclasts with a dorsal

roughness and cellular processes connecting the osteoclasts to the surface and to other osteoclasts. Many non fused OCP are also seen.

Fig. 5 TRAP-Hoechst stained OCP at 21 days of culture in differentiating medium on different substrates. Arrowheads point at TRAP-positive multinucleated cells, which were considered as osteoclasts (a,b: HA-C; c,d: HA-F; e,f: sin-HA; g,h: TCPS). Scale bar=10 micrometers. At high magnification (bottom row) some osteoclasts were seen among cells cultured on HA-C, even if less than those recognised in the TCPS and sin-HA cultures. On HA-F the cells showed a fibroblast-like morphology and differentiated osteoclasts were barely observed.

Fig. 6. Release of tartrate-resistant acid phosphatase 5b (TRAP5b) by osteoclasts on the different surfaces at 21 days of culture (units per liter).

Fig. 7 Gene expression of the osteoclast markers cathepsin K (CTSK), Matrix Metalloproteinase-9 (MMP-9) and vacuolar-ATPase (v-ATPase) by OCP at 21 days on the different surfaces.

Fig. 8. Calcium (left) and phosphorus (right) concentration in the cell culture medium after exposure to the HA disks with cells (wC) and without cells (woC) in periods of 7 days until a total of 21 days. The Ca^{++} and P^{5+} concentration of medium in contact with TCPS is included as control.

Fig. 9 TRAP staining of OCP challenged with extracts for 14 days. Arrowheads point at TRAP-positive multinucleated cells, which were considered as osteoclasts (a: HA-C; b: HA-F; c: sin-HA; d: TCPS). Scale bar=10 micrometers. Many large osteoclasts were seen among cells cultured on HA-C, similar to those recognised in the TCPS and sin-HA cultures. On HA-F OCP had a fibroblast-like morphology and differentiated osteoclasts were barely observed.

Fig. 10 Gene expression of the osteoclast markers cathepsin K (CTSK), matrix metalloproteinase-9 (MMP-9) and vacuolar-ATPase (v-ATPase) by OCP at 21 days of exposure of OCP to the different extracts.

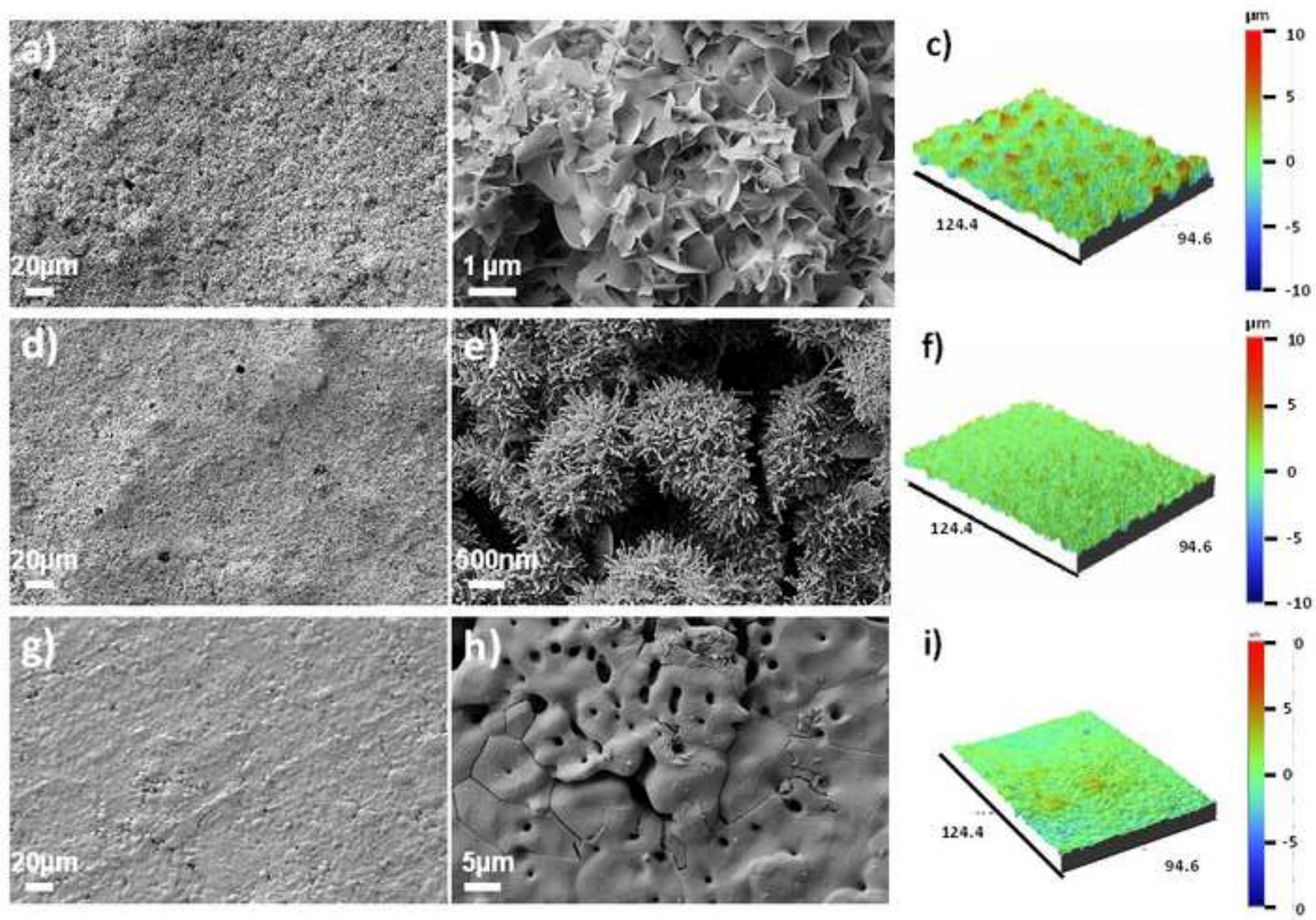


Figure 1

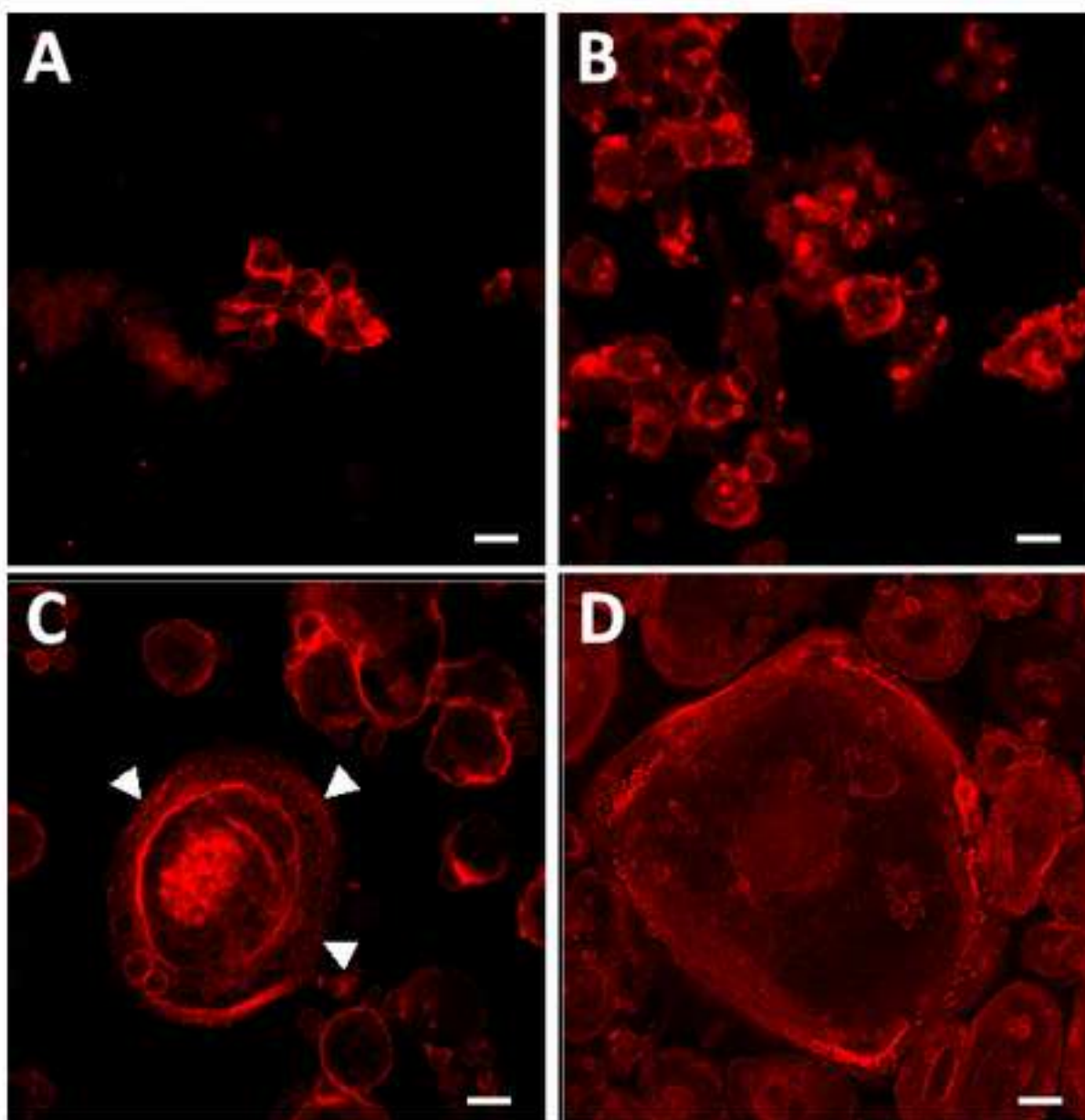


Figure 2 - new

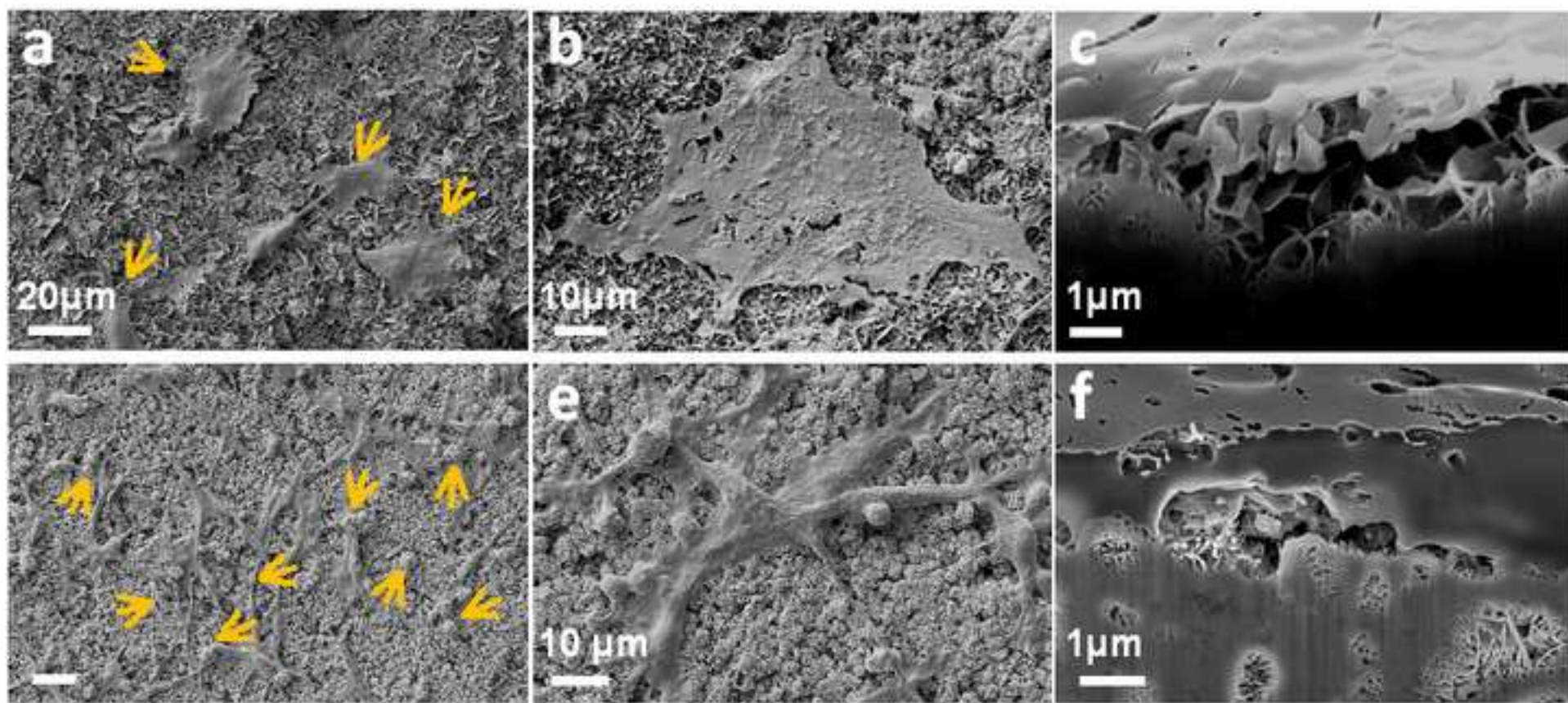


Figure 3 - new

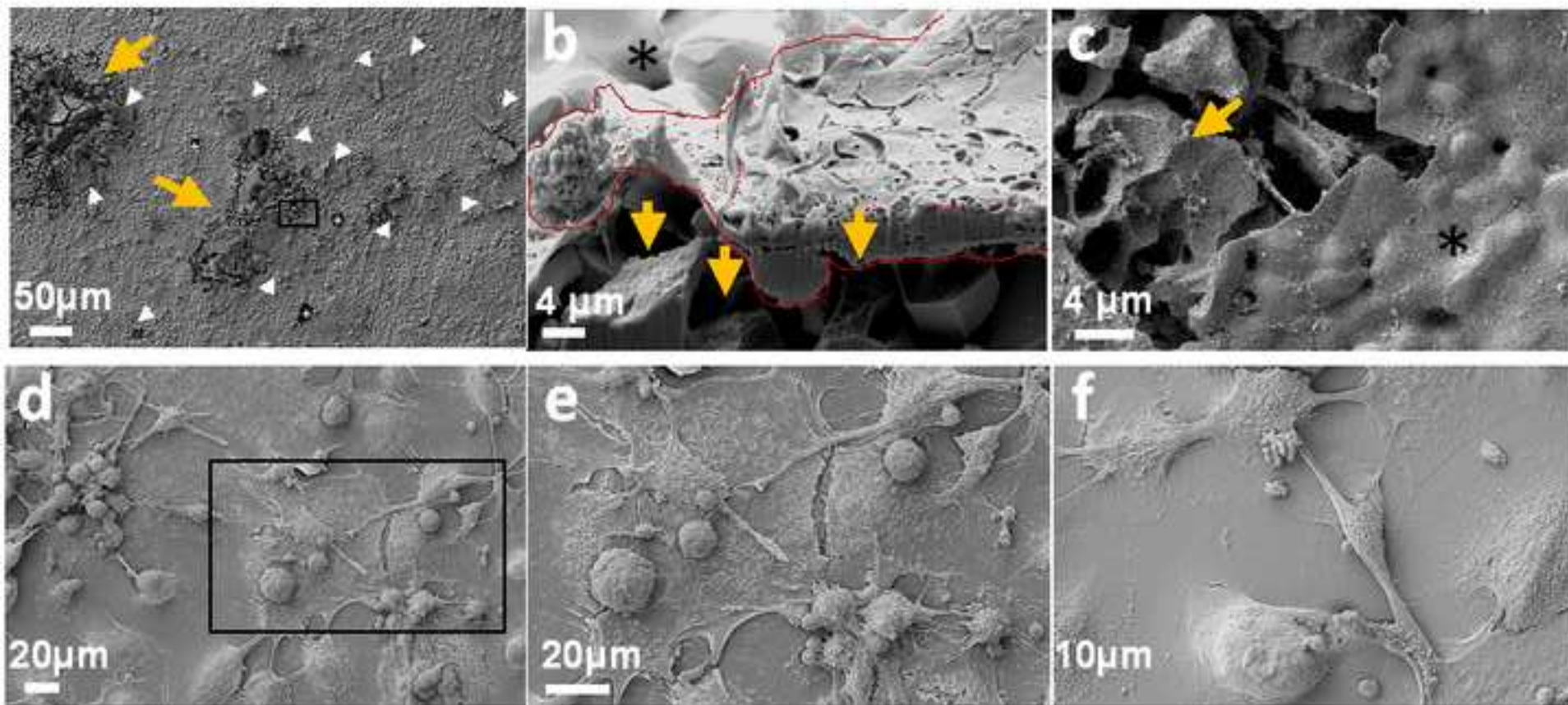
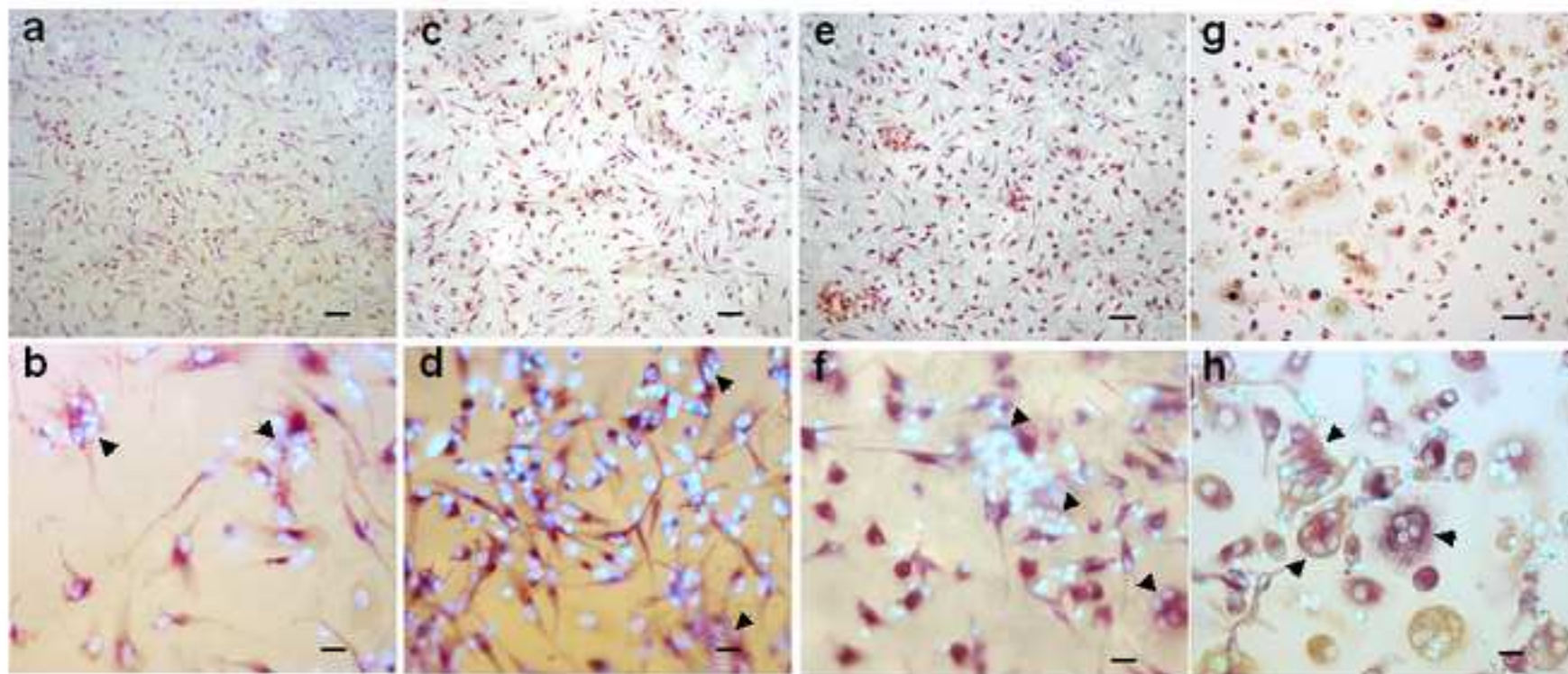
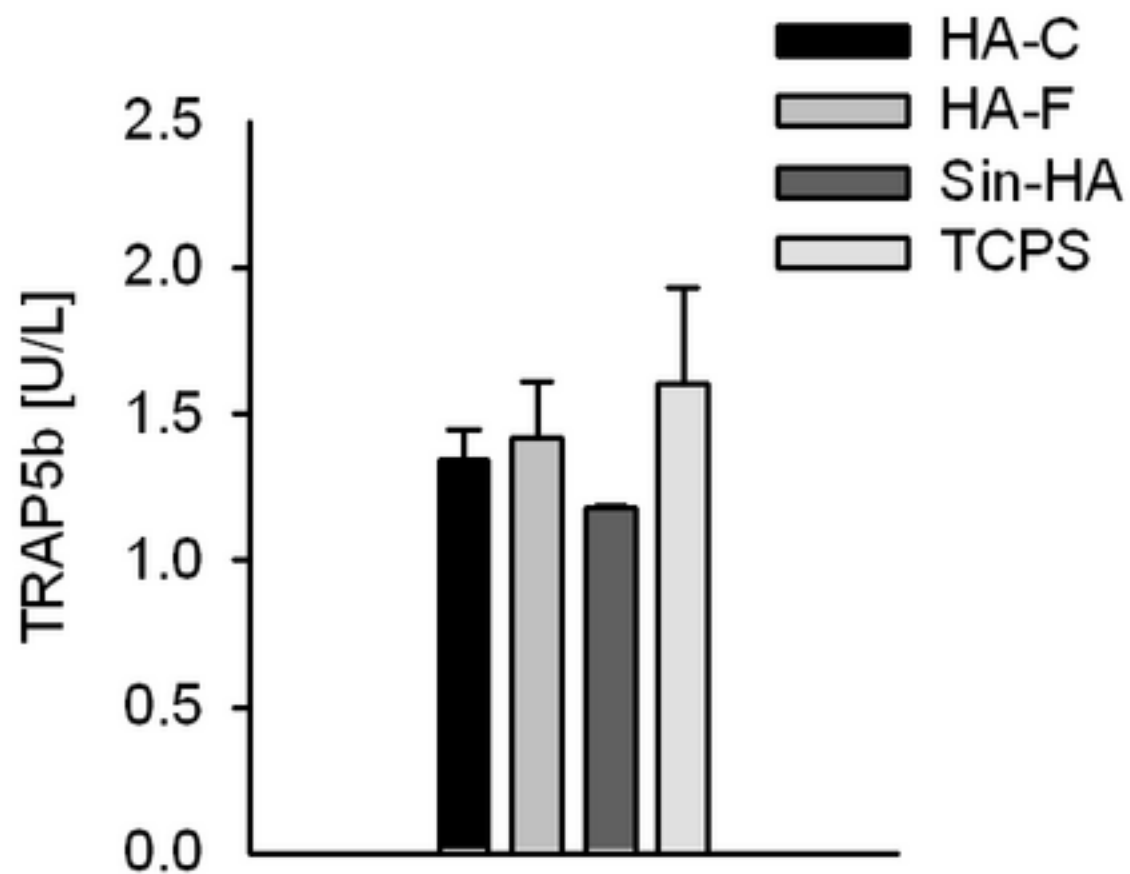


Figure 4 - new





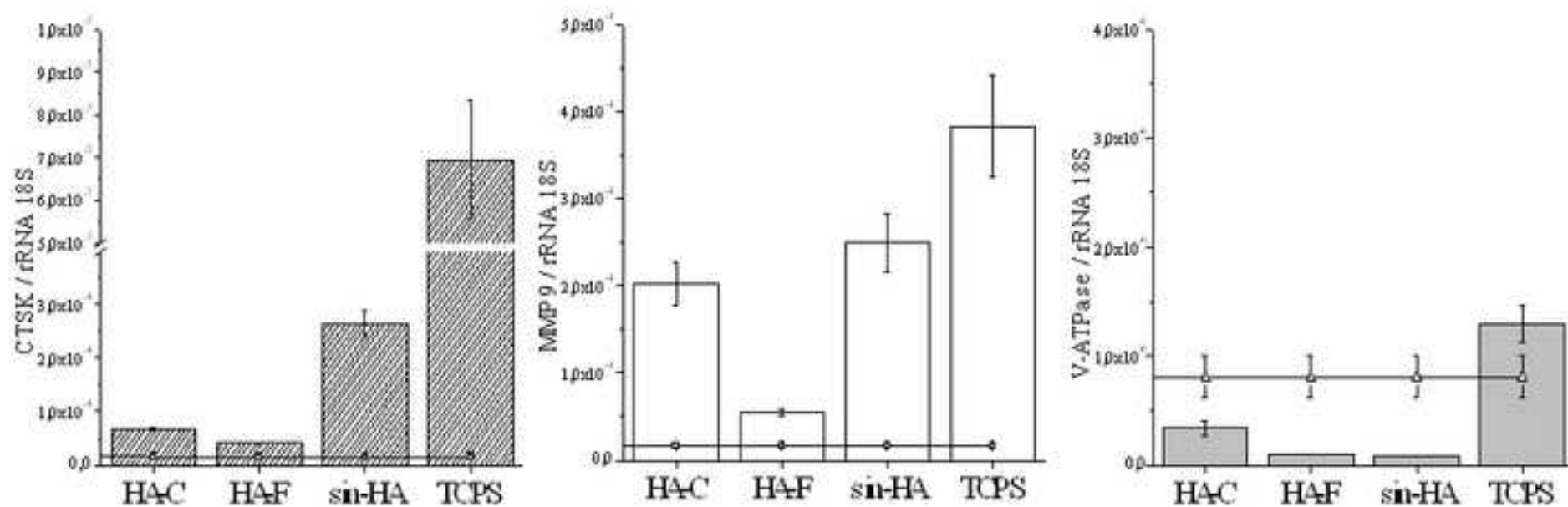


Figure 7 - new

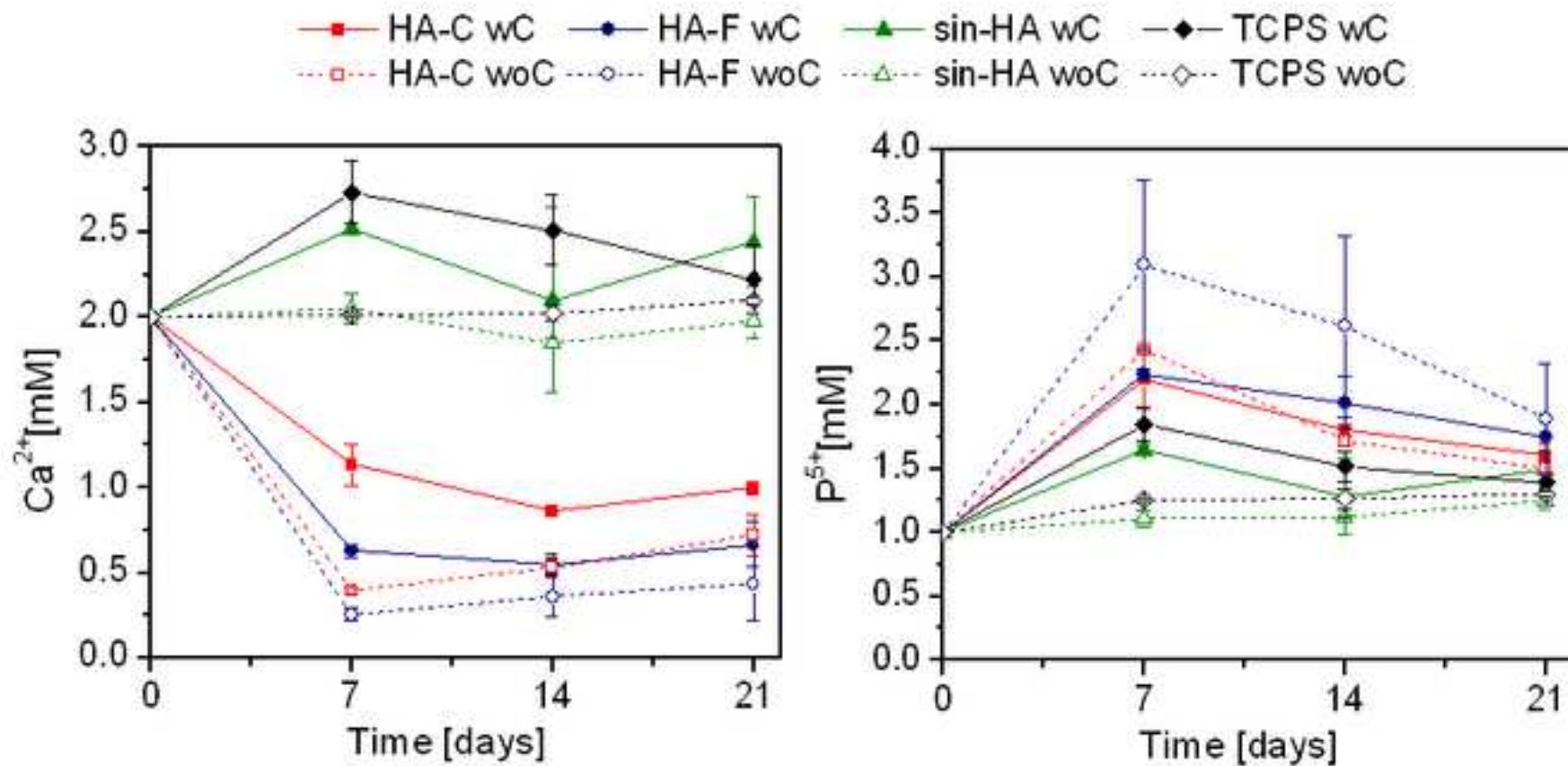
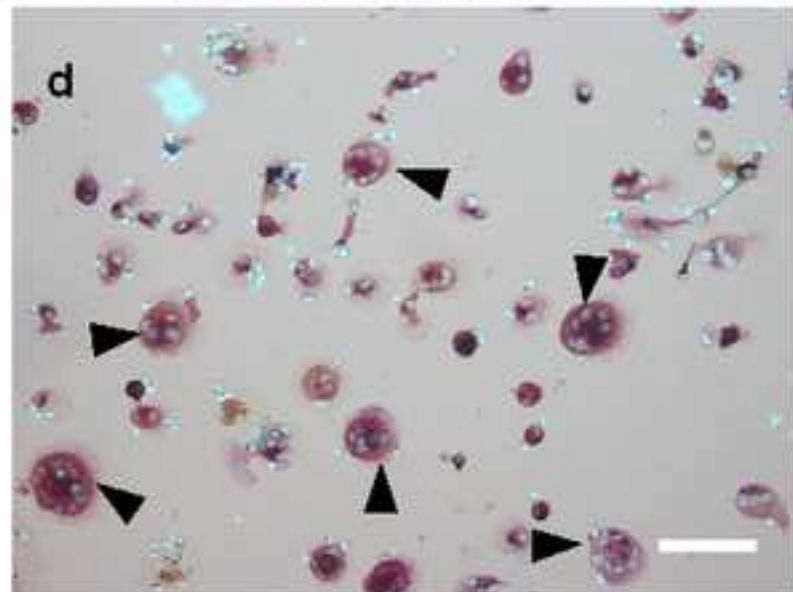
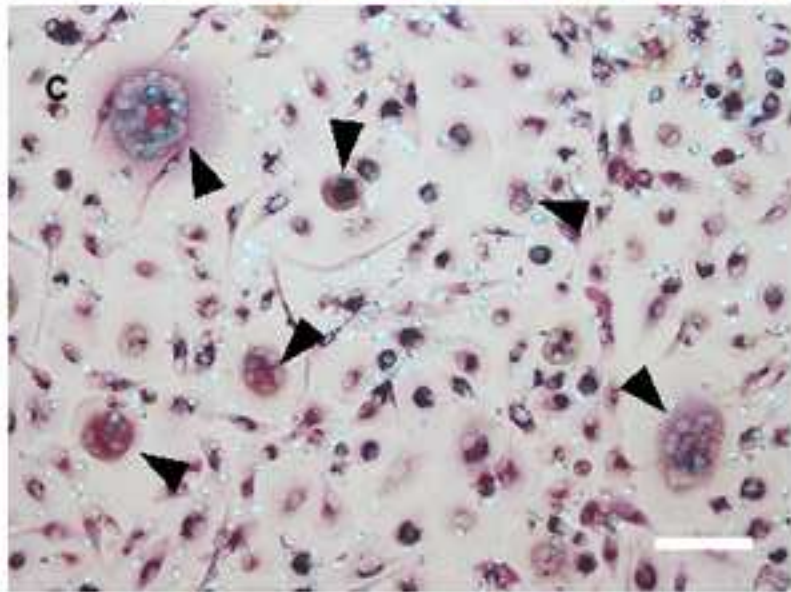
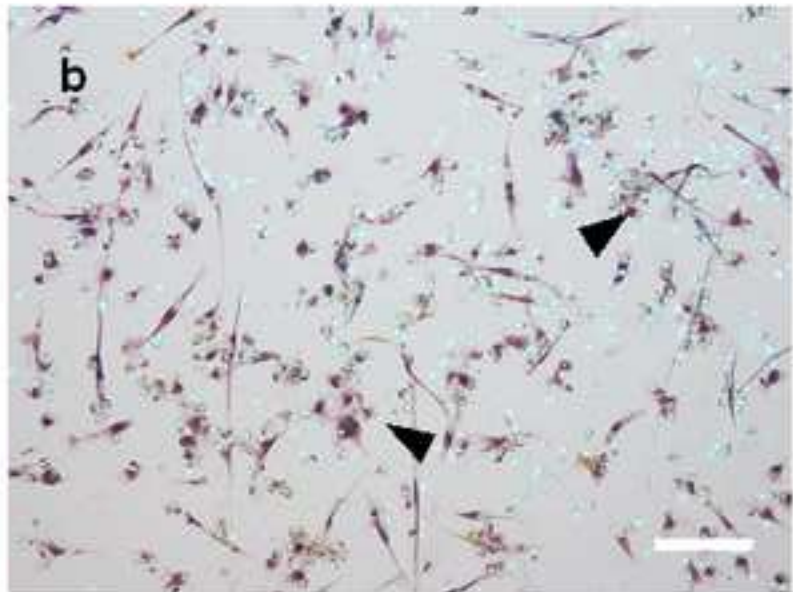
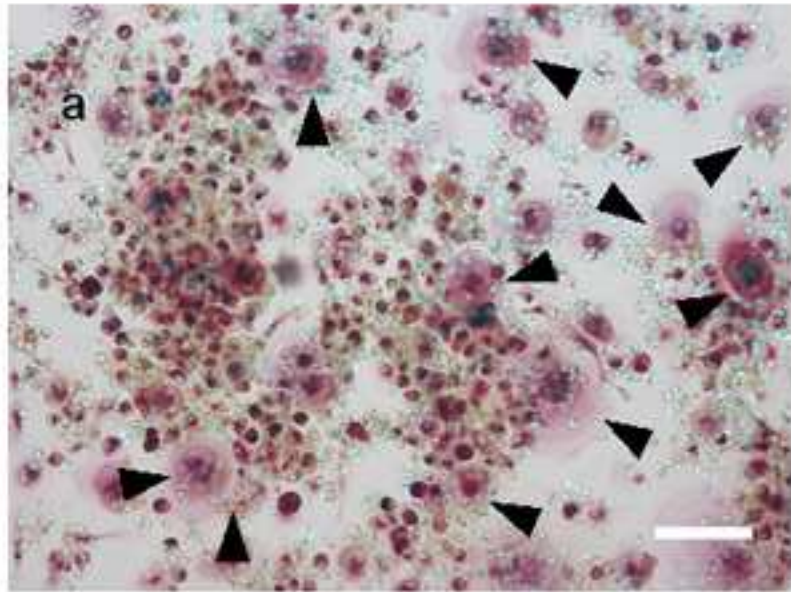


Figure 8 - new



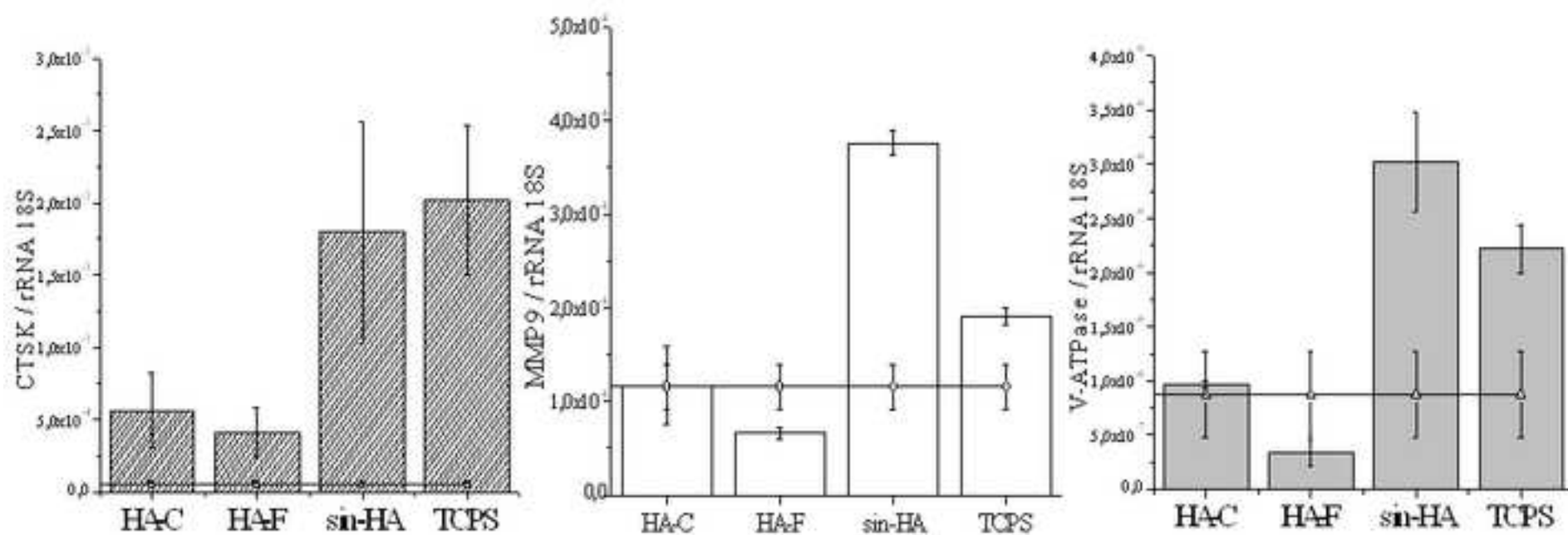
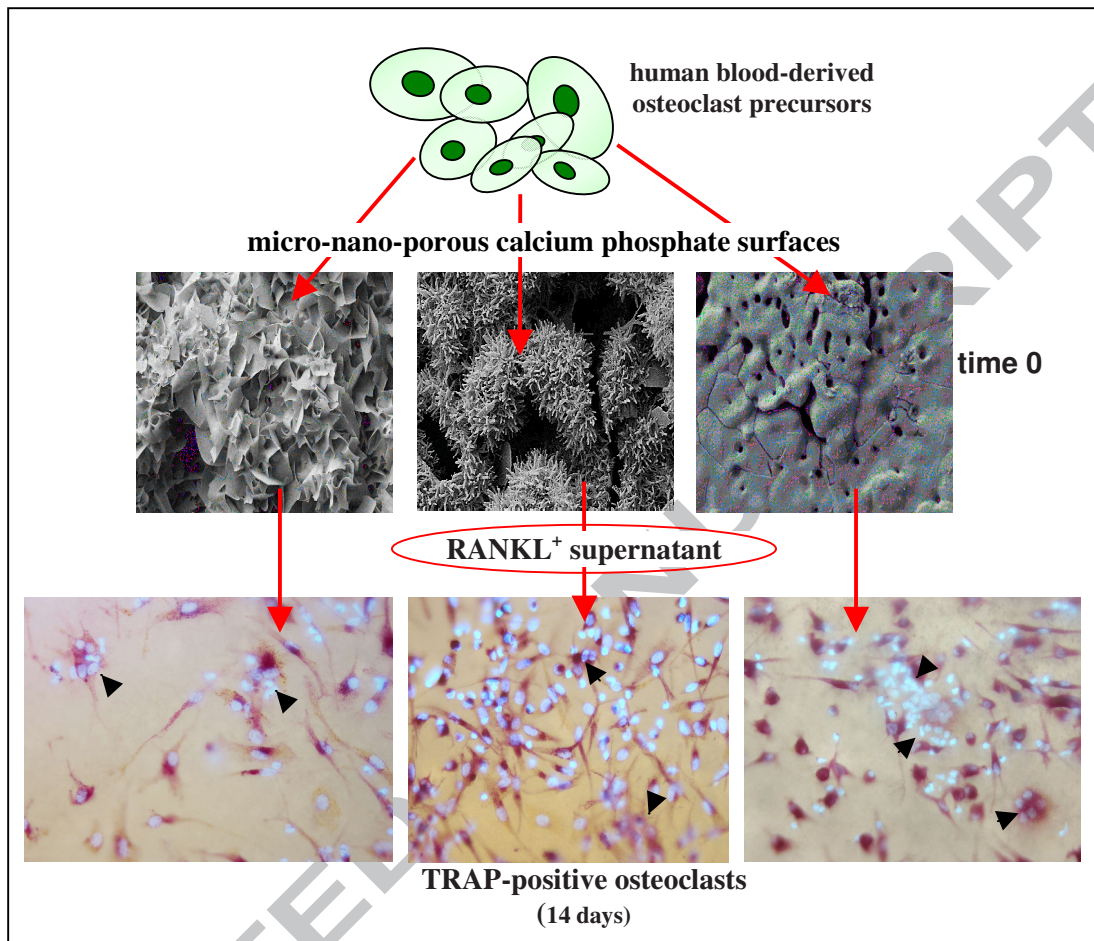


Figure 10 - new

HUMAN OSTEOCLASTS on CaP SURFACES



Gene name	Gene ID	Forward	Reverse
18S ribosomal RNA	rRNA 18s	5'-GCAATTATTCCTCATGAACG-3'	5'-GGGACTTAATCAACGCAAGC-3'
Cathepsin K	CTSK	5'-GGATATGTTACTCCTGTCAAAAATCA-3'	5'-TGCCAGTTTTCTTCTTGAGTTG-3'
Matrix metalloproteinase 9	MMP9	5'-GAACCAATCTCACCGACAGG-3'	5'-GCCACCCGAGTGAACCAT-3'
Vacuolar- ATPase	V-ATPase	5'-ATGGGGCCTCAGAGAGGA-3'	5'-GGCACCTGCCACAAAGTT-3'

Table 1. Primer sequences of target genes

OSTEOCLAST DIFFERENTIATION FROM HUMAN BLOOD PRECURSORS ON BIOMIMETIC CALCIUM-PHOSPHATE SUBSTRATES

STATEMENT OF SIGNIFICANCE

The novelty of the paper is the differentiation of human blood-derived osteoclast precursors, instead of mouse-derived macrophages as used in most studies, directly on biomimetic micro-nano structured HA-based surfaces, as triggered by osteoblast-produced factors (RANKL/OPG), and influenced by chemistry and topography of the substrate(s). Biomimetic HA-surfaces, like those obtained in calcium phosphate cements, are very different from the conventional calcium phosphate ceramics, both in terms of topography and ion exchange. The role of these factors in modulating precursors' differentiation and activity is analysed. The system is closely reproducing the physiological process of attachment of host cells and further maturation to osteoclasts toward resorption of the substrate, which occurs in vivo after filling bone defects with the calcium phosphate grafts.